JTTEE5 1:75-82

Studies on the Thermal Spraying of Apatite Bioceramics

J.G.C. Wolke, J.M.A. de Blieck-Hogervorst, W.J.A. Dhert, C.P.A.T. Klein, and K. de Groot

Hydroxylapatite (HA) coatings on metal substrates have been investigated for many years. These coatings have proved to be compatible with bone. The degree of crystallinity of HA changed, and sometimes dissociation was observed with respect to the plasma spray process. However, the plasma spray process hardly altered the crystallographic structure, with only line broadening visible. The *in vitro* solubility is dependent on the degree of crystallinity of the coating. Tensile strength measurements on the strength of the coating-substrate interface using various adhesives revealed a significant difference between epoxy resin and methacrylate. The failure mode of this tensile test was dependent on the coating thickness and surface texture (polished versus nonpolished). In animal studies, the fixation of hydroxylapatite plasma-spray coated cylinders as well as noncoated Ti-6Al-4V cylinders (Ti) in cortical bone was evaluated using push-out tests. It appeared that HA-coated implants showed higher push-out strengths in the first months than the titanium implants, because of the earlier bone formation against the HA coating.

1. Introduction

THE first application of calcium phosphate materials as bone substitute or bone graft may be traced to Albee,[1] who reported that a "triple calcium phosphate" compound, used in a bone defect promoted osteogenesis, *i.e.*, new bone formation. Since then, numerous investigators have studied calcium phosphate implants for bone replacement.

Bioactive ceramics[2] can be incorporated in living bone without the presence of a fibrous tissue interlayer between the bone and the implant due to their similarity with the mineral phase of the bone. The brittleness and poor strength of bulk bioceramics require that clinical application is limited to those sites in the human body where no cyclic load-bearing forces are present.

Therefore, calcium phosphate coatings on metallic substrates have been developed.[3,4] These thin coatings (about 50 μm) on metal substrates have been applied by various techniques such as hot pressing, plasma or flame spraying, sputter deposition, frit enameling, electrophoretic deposition, and sol-gel deposition.[5] The plasma spray technique is now used widely for biomedical applications such as total joint replacements and dental root implantations. Animal experiments have shown that hydroxylapatite (HA) plasma-sprayed coatings are biocompatible when implanted in soft tissue or bone.[6-8]

Key Words: bioceramic coatings, biocompatibility tests, failure properties, fluroapatite, hydroxylapatite, phase structure

J. G. C. Wolke, Department of Biomaterials, School of Medicine, University of Leiden, Rijnsburgerew 10, 2333 AA Leiden, The Netherlands; **J. M. A. de Blieck-Hogervorst,** Department of Oral Implantology, ACTA-Vrije Universiteit, Amsterdam, The Netherlands; **W. J. A. Dhert**, Department of Biomaterials, School of Medicine, University of Leiden, The Netherlands, Division of Orthopaedic Surgery, Leiden University Hospital, The Netherlands; **C. P. A. T. Klein,** Department of Oral Implantology, ACTA-Vrije Universiteit, Amsterdam, The Netherlands; **K. de Groot**, Department of Biomaterials, School of Medicine, University of Leiden, The Netherlands.

In the present study, the results of a study on some physical aspects of plasma-sprayed hydroxylapatite and fluorapatite (FA) coatings will be presented. The coatings were examined by measurements on X-ray diffraction, bonding strength, powder morphology, and solubility in various buffers. In addition, the results will be discussed in relation to previous *in vivo* push-out studies, as well as in relation to the theoretical background of this push-out test.

The Appendix at the end of this article lists and defines some of the terms that are used in this discussion.

2. Materials and Methods

2.1 *Starting Powders for the Plasma Spray Process*

Hydroxylapatite powder was obtained from Merck Inc. Fluorapatite was prepared by mixing 93.05 g tricalcium phosphate with 7.80 g calcium fluoride; *i.e.*, in stoichiometric proportions. The powders were granulated (1 to 2 mm) and sintered under an inert atmosphere. Thereafter, the granules were crushed, milled, and sieved. For HA and FA, two particle size distributions were used in the plasma spray process: 1 to 45 μm (designated as HA-45 and FA-45) with a mean particle size of 24 and 25 μm, respectively, and 1 to 125 μm (designated as HA-125 and FA-125), with a mean particle size of 60 and 64 μm, respectively.

Table 1 Plasma Spray Parameters

Arc current	400 A
Arc voltage	62 V
Arc gas	Nitrogen (44.8 l/min)
Powder gas	Nitrogen (5.1 l/min)
Gun speed	10 cm/sec
Powder transport	10 to 15 g/min
Cooling	Air
Substrate distance	8 cm

Table 2 Surface Roughnesses of Substrate and Coating

Surface	Roughness, μm
Ti-6Al-4V (grit blasted)	4.5 to 5.0
HA-45 (coating)	6.8 to 7.3
HA-125 (coating)	7.8 to 9.0
FA-45 (coating)	6.5 to 7.1

Table 3 Tensile Strength and Failure Mode of HA Coatings Using Various Adhesives

Adhesive	Strength MPa	Failure mode	No. of tests
Araldit AV 118	60.8	100% glue/HA	5
3M 2241	38.3	100% glue/HA	5
Lee Insta-Bond	5.4	100% HA/Ti	3
Concise	11.7	100% HA/Ti	3

2.2 *Plasma Spray Parameters*

For the plasma spray process, a Metco MN system was used. The conditions for the plasma spray process are listed in Table 1.

2.3 *Substrates*

Cylindrical rods of Ti-6Al-4V (referred to as Ti) alloy were manufactured. All plugs measured 7.0 mm in length. The diameter of the plugs that were plasma-spray coated with HA was 5.0 mm, and the diameter of the plugs that remained uncoated (Ti) was 5.1 mm. All plugs were grit blasted, cleaned ultrasonically, and dried at 100 °C. The 5.0-mm plugs were plasma sprayed with HA until a coating thickness of 50 μm was reached. Then all plugs were again cleaned ultrasonically in 100% ethanol to remove any loose particles and then dried at 50 °C.

Stainless steel plates were used (50 by 20 by 2 mm) for X-ray diffraction and solubility tests. The same grit blasting, cleaning, and drying procedures were used as for the HA plug specimens. Several plates were heat treated for 1 hr at 600 °C in an inert furnace after plasma spraying.

2.4 *Surface Characterization*

The substrate surfaces were characterized by means of roughness measurements with a Taylor-Hobson profilometer.

2.5 *Tensile Bond Strength*

Tensile strength was determined on the coated Ti-6Al-4V rods, which were glued together with various epoxy glues (Araldit AV 118, heated for 12 hr at 120 °C; or 3M 2214 heated for 1 hr at 120 °C) or cold curing methacrylate glues (Concise or Lee cured for 15 min at 25 °C). This test was similar to the ASTM C633-69 test, and the major difference was the change in diameter of the plug.[9] Experiments were performed using a Hounsfield mechanical testing machine with a crosshead speed of 5 mm/min. The thickness of the coatings and surface texture (polished versus unpolished) were varied.

Table 4 Tensile Strength and Failure Mode of HA Coating Versus Thickness

Thickness, μm	Strength, MPa	Failure mode	No. of tests
40	66.8	100% glue/HA	5
80	60.7	100% glue/HA	5
120	45.3	100% HA/Ti	2
		100% glue/HA	1

Table 5 Tensile Strength and Failure Mode of Polished and Unpolished HA-Coated Surfaces

Surface	Strength, MPa	Failure mode	No. of tests
HA	60.8	100% glue/HA	5
HA polished	53.0	55% glue/HA	5

2.6 *X-Ray Diffractometry*

X-ray diffraction patterns were measured on the plates using the following equipment and operational parameters: Philips automatic vertical X-ray powder diffractometer PW 1050, measuring system PW 1710, CuK_α radiation (3-kW HV generator PW 1130/90, 45 kV/33 mA; 0.018-mm nickel CuK_β filter), divergence slit 1°, receiving slit width 0.1 mm, xenon sealed proportional detector, and pulse height selection.

2.7 *Solubility Test*

Solubility experiments were performed on the plates using Michaelis and Gomori's buffer solutions at pH 7.2 and a temperature of 37 °C. Details on the preparation of these solutions are provided in Ref 7. The follow-up period was 3 months. The calcium and phosphate concentrations in the solutions were measured using a Varian AAS and a Vitatron spectrophotometer.

2.8 *In Vivo Experiments*

Healthy dogs were used for the experiments. The implants were inserted into the femoral bone. The implants were left *in situ* for 3, 5, 15, and 25 months.

3. Results

3.1 *Roughness Values*

The roughness values measured for the coated and blasted surfaces are presented in Table 2. The roughness values are similar for the various coated surfaces.

3.2 *Tensile Bond Strength*

Tensile strengths were measured only for the HA-coated specimens using the various adhesives and Araldit AV 118 as a function of coating thickness or surface texture. The tensile strengths of a typical HA coating are presented in Table 3. The coating thickness varied from 45 ± 5 μm.

The epoxy-based glues result in much higher strength values than cold curing (dental) cements. In addition, the failure mode

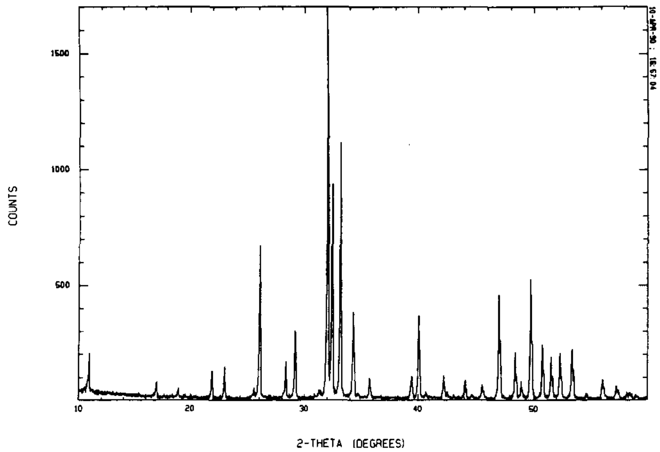

Figure 1 X-ray diffraction pattern of sintered HA feedstock powder.

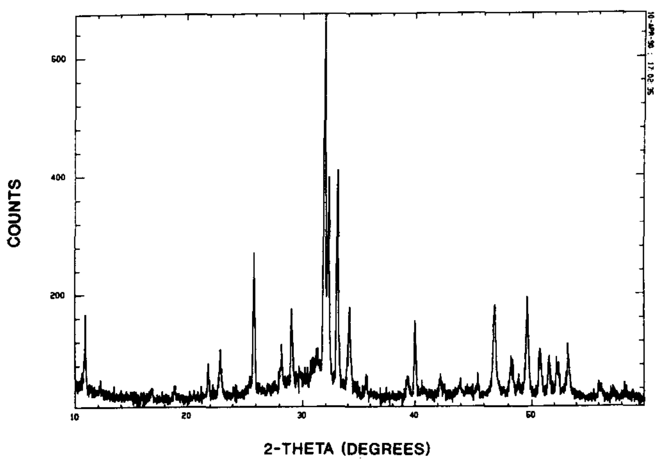

Figure 2 X-ray diffraction pattern of HA-125 coating. The plasma gas is nitrogen.

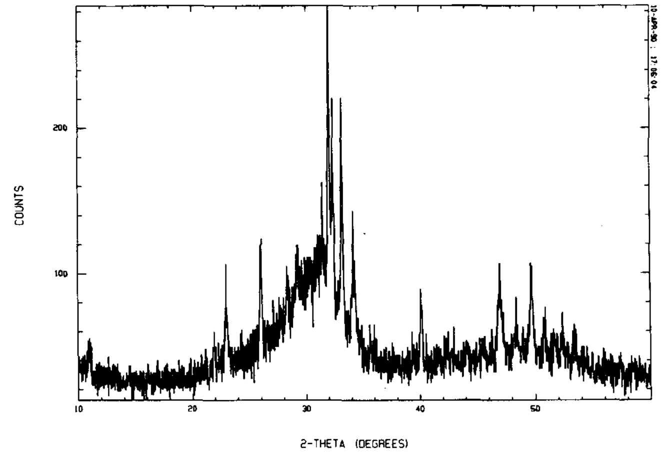

Figure 3 X-ray diffraction pattern of HA-45 coating. The plasma gas is nitrogen.

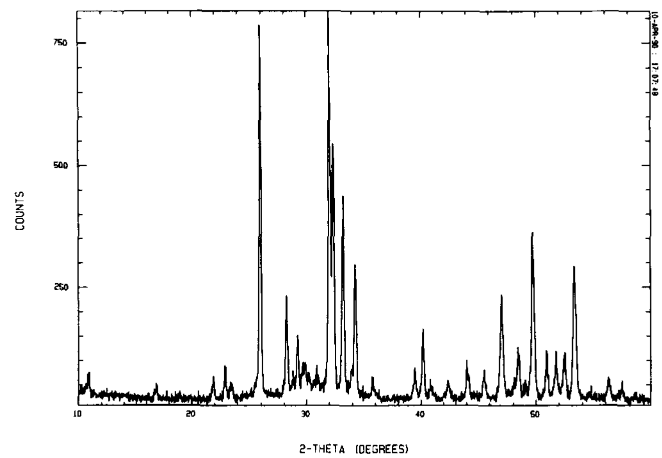

Figure 4 X-ray diffraction pattern of FA-45 coating. The plasma gas is nitrogen.

for the epoxy glues differs from those found in the dental cements, where the locus of failure changes from the substrate/coating interface to the glue line of the specimen assembly. The Araldit AV 118 epoxy was chosen for further tests, because it exhibited the greatest adhesion strength. The FA coatings tested for adhesion by this method exhibited similar tensile strength as the HA coatings.

For various coating thicknesses, the tensile strengths glued with Araldit AV 118 are presented in Table 4. Tensile strength measurements on the polished and unpolished HA-coated surfaces glued with Araldit AV 118 are presented in Table 5.

3.3 *X-Ray Diffraction*

Figure 1 shows the X-ray diffraction pattern of sintered HA feedstock powder. Minimal line broadening can be seen, which indicates a well-crystallized material. Figure 2 shows the XRD pattern of HA-125 sprayed with nitrogen as the plasma gas. It can be seen that plasma spraying does not significantly alter the crystallographic structure, and a little line broadening is visible.

Figure 3 shows the XRD patterns of a plasma-sprayed HA-45 coating; the structure of the coating consists almost entirely of amorphous phases. The authors believe this is caused by complete melting of the small particles, which results in an amorphous coating. However, as shown in Fig. 4, a FA coating sprayed with the same particle size distribution produces a crystalline coating comparable with the 1 to 125 μm HA coating (Fig. 2). Thus, plasma spraying of this material decreases the degree of crystallinity. The ratio of the intensity of the peaks is changed due to the orientation of the crystals during the cooling process (the peak at 25.7° 2θ is increased).

Figure 5 shows the XRD pattern of HA-45 after heat treatment for 1 hr at 600 °C in an inert environment that prevents oxidation of the metal. This heat treatment increases the crystallinity, and the amorphous phase is removed, as observed by comparison with Fig. 3. Figure 6 shows the XRD pattern of an as-received HA-125 plasma-sprayed coating after an *in vitro* solubility test for 3 months in Michaelis buffer. An increase in crystallinity can be observed, and after this incubation time, no amorphous phase is present.

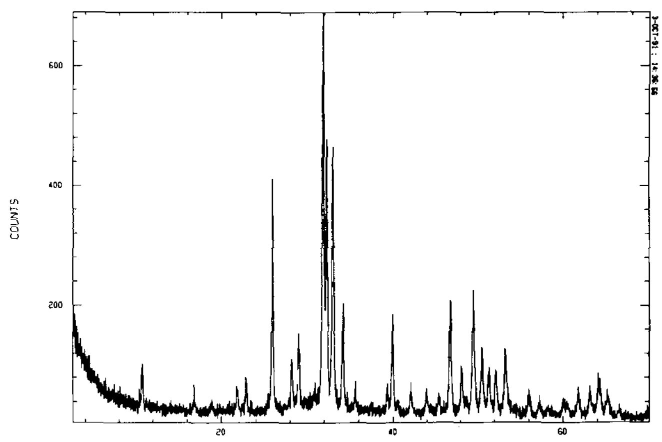

Figure 5 X-ray diffraction pattern of HA-45 coated plate treated for 1 hr at 600 °C.

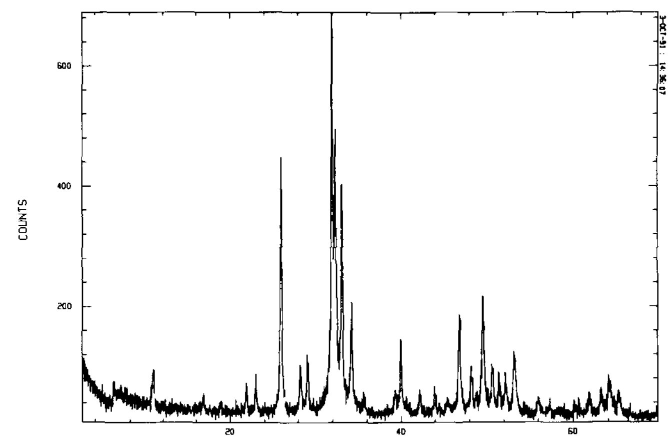

Figure 6 X-ray diffraction pattern of HA-125 coated plate after incubation for 3 months in Michaelis buffer with pH 7.2 at 37 °C.

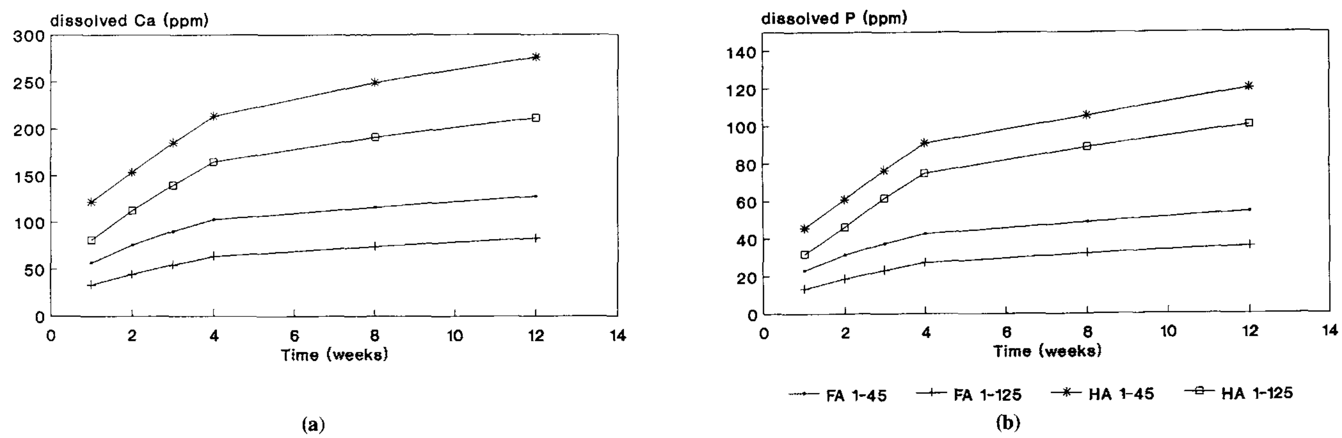

Figure 7 Calcium (**a**) and phosphate (**b**) release of bioceramic coating in Gomori buffer with pH 7.2 at 37 °C.

3.4 *Solubility*

Figures 7 and 8 show the phosphate and calcium concentration in Gomori's and Michaelis buffers. Calcium and phosphate concentrations due to dissolution of the coatings decreased in the order HA-45 > HA-125 > FA-45 > FA-125. Figure 9 shows the solubility behavior of amorphous HA coating for 3 months in Gomori's buffer at 37 °C. The solubility decreases by a factor of 2 for a heat treated coating. The decrease is not as great when the coating is of mixed amorphous/crystalline nature (Fig. 10). In general, it is a good alternative to decrease the solubility behavior of a coating.

3.5 *In-Vivo Experiment*

Figure 11 shows that the titanium plugs implanted in the femur of a dog have a lower push-out strength than a HA-coated implant. Hydroxylapatite exhibits a higher bonding strength in the first months.

Figure 12 shows a back-scattered electron image of a HA coating after 5 months implantation in the femur of a dog, with special attention to the fracture site from a push-out test. The bone apposition is good, and fracture is located at the titanium/HA interface. Thus, the bone/coating interface is stronger than the coating titanium interface.

Figure 13 shows the section of a HA coating implant at 25 months and illustrates good bone apposition, although the coating has completely resorbed. Figure 14 shows a titanium implant after 25 months implantation, where a fibrous tissue interlayer is formed and there is no bone apposition against the implant.

4. Discussion

The surface roughness of the coatings did not depend on the chemical composition of the coating powder, but only on their particle distribution (other parameters being similar). Tensile strength measurements indicated that various adhesives exhibited different tensile strengths and failure modes for the coating. An important phenomenon is that the dental adhesives are able to pull off the coating from the titanium, although they have a very low tensile strength. Although the epoxy adhesives have very high tensile strengths, no coating is removed from the met-

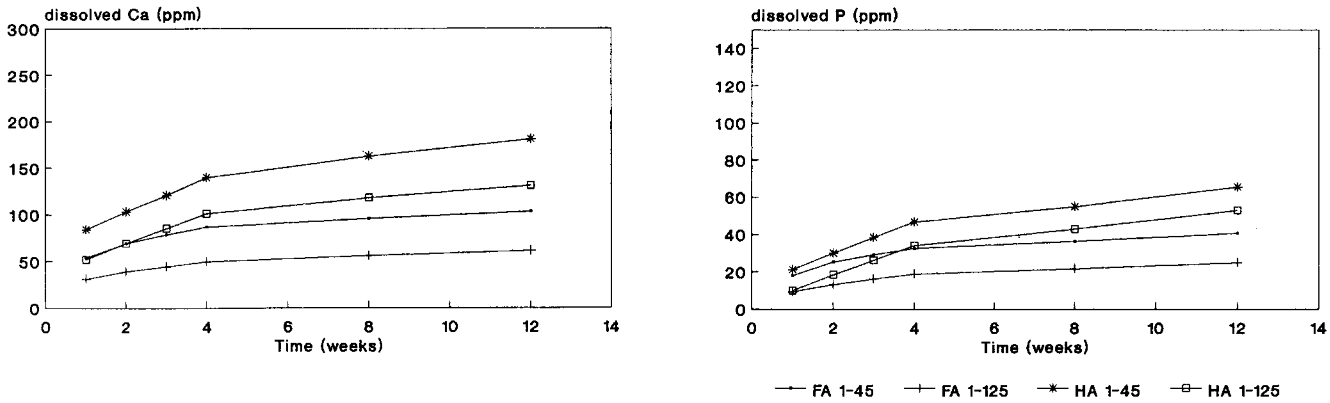

(a) (b)

Figure 8 Calcium (a) and phosphate (b) release of bioceramic coating in Michaelis buffer with pH 7.2 at 37 °C.

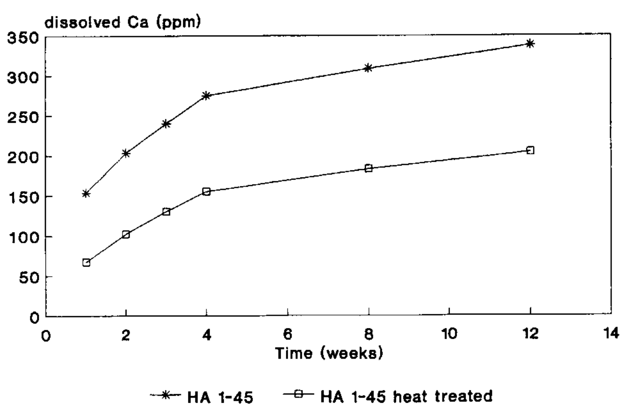

Figure 9 Calcium ion release of amorphous and heat treated HA coatings in Gomori's buffer (pH 7.2 at 37 °C).

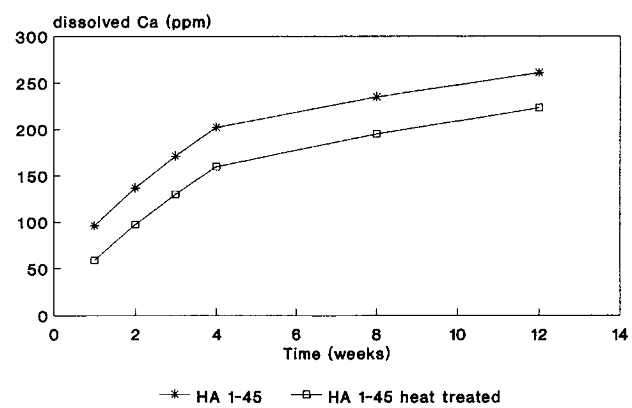

Figure 10 Calcium ion release of amorphous/crystalline and heat treated amorphous/crystalline HA coatings in Gomori's buffer (pH 7.2 at 37 °C).

al. An explanation for the results of the dental adhesives could be that the low viscous liquid in the dental adhesive penetrates quickly through the coating layer and alters the thermal spray coating while setting. The epoxy adhesives, on the other hand, show failure at the interface between the adhesive and coating.

These experiments show that different adhesives exhibit different failure modes and tensile strengths. Thus, to compare data from different laboratories, it is necessary to take into account the experimental techniques.

The thickness of the coating influenced the failure modes, probably because alignment of the specimen assembly in the tensometer plays a more important role with thicker coatings. This is in agreement with the literature, where it is shown that glassy films have a strength that is inversionally related to thickness, *i.e.*, thin films are stronger than thicker ones (for thicknesses <200 μm).[10] Polishing the coated surface produced a reduction in tensile strength, and failure occurred more in the metal/ceramic interface.

X-ray diffraction shows that, depending on the nature of the plasma flame, a crystalline phase can be obtained. It can be noted that a very hot flame produces an amorphous coating with the formation of calcium oxide. After incubation *in vivo* or *in vitro*, the amorphous phase was either resorbed through physicochemical dissolution or changed via a phase transition from an amorphous to a crystalline structure.

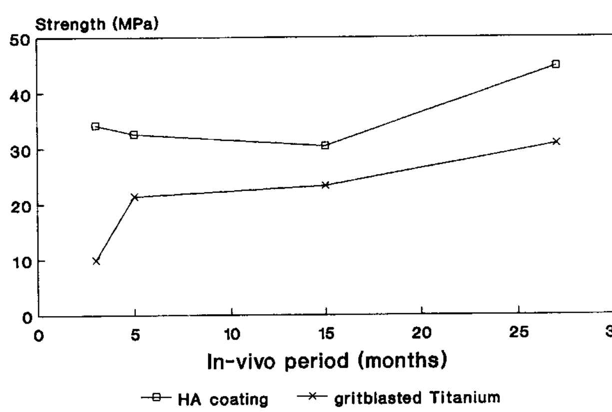

Figure 11 Push-out strength of grit-blasted titanium and HA-coated plugs implanted in the femur of a dog.

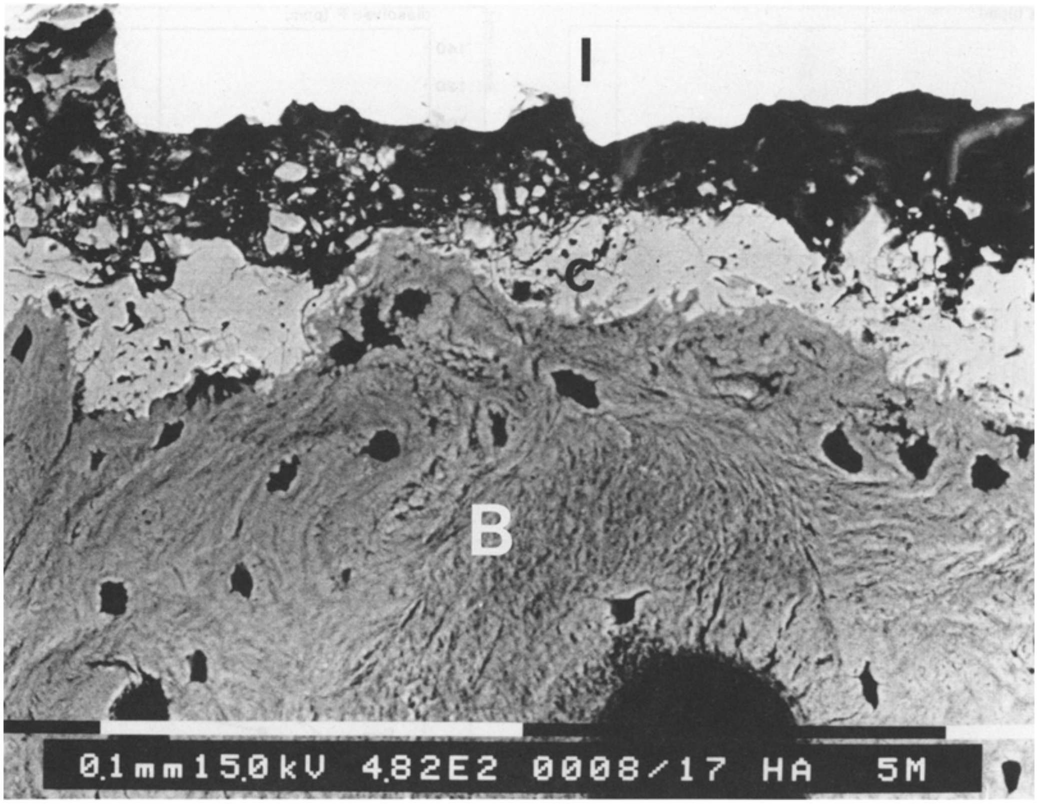

Figure 12 Back-scattered electron image of a HA coating after 5 months implantation. (I = implant, C = coating, B = bone.)

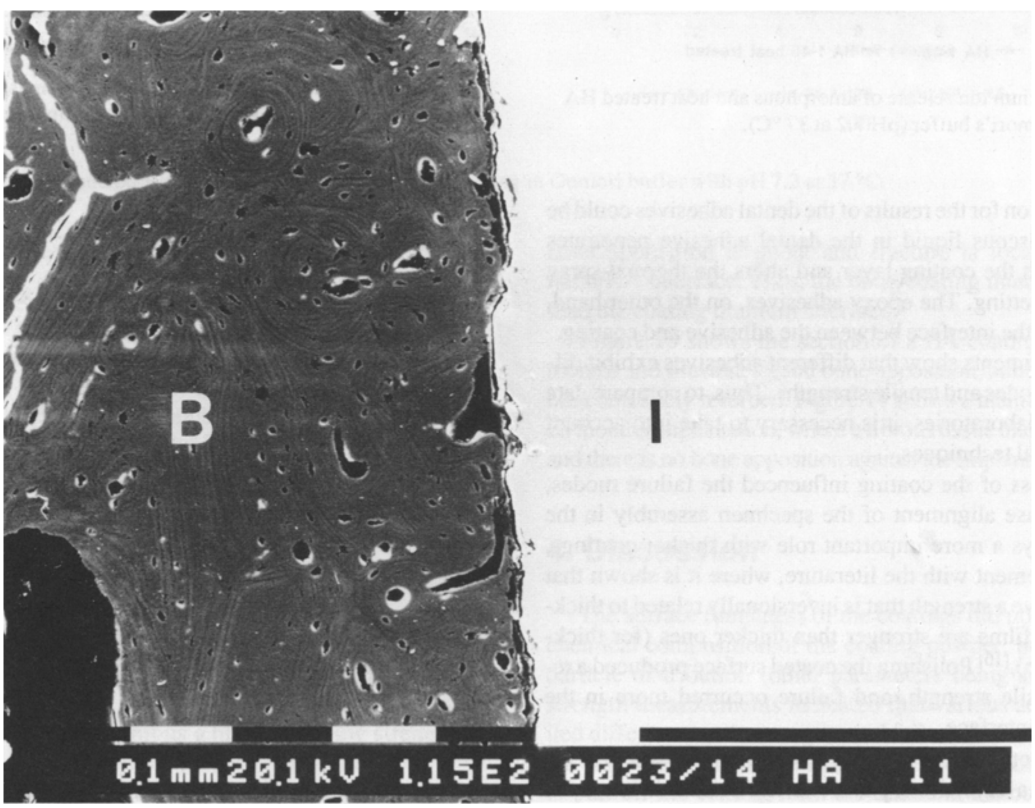

Figure 13 Back-scattered electron image of a HA coating implant after 25 months implantation. (I = implant, B= bone.)

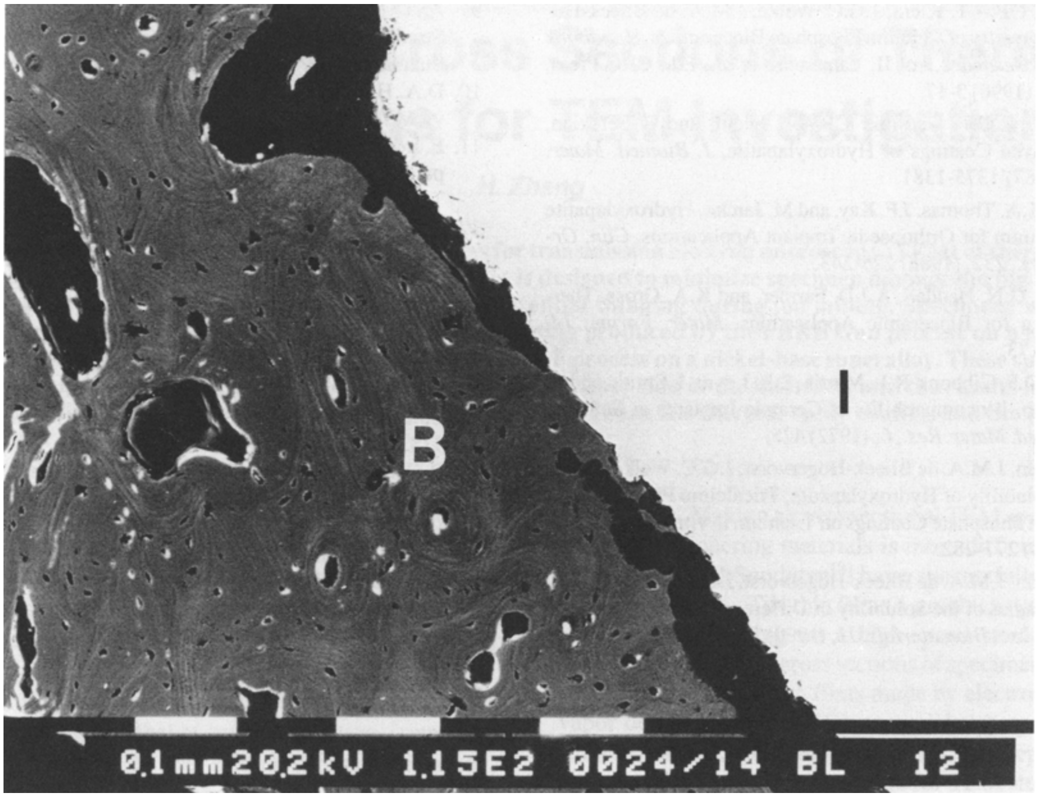

Figure 14 Back-scattered electron image of a titanium implant after 25 months implantation. (I = implant, B = bone.)

A HA coating sprayed with a particle distribution of 1 to 45 μm produces an entirely amorphous phase, and this coating dissolves faster. Heat treatment after plasma spraying increases crystallinity and decreases solubility of the coating. The thermal stability of fluorapatite at elevated temperatures is superior to that of hydroxylapatite, and therefore, a FA coating has a higher degree of crystallinity compared to a HA coating. [11]

The solubility tests show clearly that *in vitro* FA is less soluble than HA. It must be emphasized that *in vitro* solubilities are generally not predictive for *in vivo* behavior, as shown by Ramselaar *et al.*, [12] animal studies by Klein *et al.*, [8] and Dhert *et al.*[13] However, at least for FA and HA, the *in vitro* findings closely parallel the *in vivo* results examined in the present work.

The animal studies showed some dissolution of the HA coating; however, push-out studies show that the bone fixation to coated surfaces stays high and is superior to uncoated surfaces.[14,15]

5. Summary

Apatite coatings of hydroxylapatite and fluorapatite are characterized in terms of crystallographic structure, bonding strength, thickness, and *in vitro* and *in vivo* degradation behavior. Although HA coatings degrade gradually, FA coatings are more stable after incubation in physiological fluid and after implantation under unloaded conditions.

Push-out studies, however, showed that the high strengths of the HA coating did not change after gradual dissolution of the coating. Furthermore, because uncoated (and unloaded) titanium implants become bonded to bone after about 1 year, the conclusion is that apatite coatings are most important during the healing phase.

Acknowledgments

The authors wish to acknowledge CAM-Implants B.V. for the use of its facility, Mr. J. Koerts for his assistance, and Mr. W. Molleman (Laboratory for Crystallography, University of Amsterdam) for the X-ray diffractograms.

Appendix: A Selection of Biomaterial Terms

Apposition: Abutment of bone against implant material.

Fluorapatite: $Ca_5(PO_4)_3F$.

Hydroxylapatite: $Ca_5(PO_4)_3OH$.

Osteogenesis: Potency to form bone tissue by bone-forming cells, *i.e.*, osteoblasts.

Resorbed: Bone resorption is bone reduction by osteoclastic cells.

References

1. F.H. Albee, Studies in Bone Growth Triple Calcium Phosphate as a Stimulus to Osteogenesis, *Ann. Surg.*, *71*, (1920) 32-39 .

2. K. de Groot, C.P.A.T. Klein, J.G.C. Wolke, J.M.A. de Blieck-Hogervorst, Chemistry of Calcium Phosphate Bioceramics, *Handbook of Bioactive Ceramics*, vol II, Yamamuro *et al.*, Ed., CRC Press, Boca Raton, (1990) 3-17.
3. K. de Groot, R.G.T. Geesink, C.P.A.T. Klein, and P. Serekian, Plasma Sprayed Coatings of Hydroxylapatite, *J. Biomed. Mater. Res., 21*, (1987) 1375-1381.
4. S.D. Cook, K.A. Thomas, J.F. Kay, and M. Jarcho, Hydroxylapatite Coated Titanium for Orthopaedic Implant Applications, *Clin. Orthop. Rel. Res., 232*, (1988) 225-243.
5. C.C. Berndt, G.N. Haddad, A.J.D. Farmer, and K.A. Gross, Thermal Spraying for Bioceramic Applications, *Mater. Forum, 14*, (1990) 161-173.
6. S.D. Davis, D.F. Gibbons, R.L. Martin, S.R. Levitt, I. Smith, and R. V. Harrington, Biocompatibility of Ceramic Implants in Soft Tissue, *J. Biomed. Mater. Res., 6*, (1972) 425.
7. C.P.A.T. Klein, J.M.A. de Blieck-Hogervorst, J.G.C. Wolke, and K. de Groot, Solubility of Hydroxylapatite, Tricalcium Phosphate and Tetracalcium Phosphate Coatings on Titanium in vitro, *Adv. Biomater., 9*, (1990) 277-282.
8. C.P.A.T. Klein, J.M.A. de Blieck-Hogervorst, J.G.C. Wolke, and K. de Groot, Studies of the Solubility of Different Calcium Phosphate Particles in vitro, *Biomaterials, 11*, (1990) 509-513.
9. ASTM C633, "Standard Method of Test for Adhesion or Cohesive Strength of Flame Sprayed Coatings," 19th Annual Book of ASTM Standards, Part 17, ASTM, Philadelphia, (1969) 636-642.
10. D.A. Hardwick, The Mechanical Properties of Thin Films: A Review, *Thin Solid Films, 154*, (1987) 109-124.
11. E. Lugscheider, T. Weber, and M. Knepper, "Production of Biocompatible Coatings of Hydroxylapatite and Fluorapatite," National Thermal Spray Conference, Cincinnati, (1988) 332-343.
12. M.M.A. Ramselaar, J.R. de Wijn, and J. van Mullen, "Resorption of 4 Ca Phosphates, in vitro Rates and Tissue Reactions," Books of Abstract, C1-6, 8th European Conference on Biomaterials, European Society for Biomaterials, Heidelberg, 7-9 Sep (1989).
13. W.J.A. Dhert, C.P.A.T. Klein, J.G.C. Wolke, E.A. van der Velde, K. de Groot, and P.M. Rozing, A Mechanical Investigation of Fluorapatite, Magnesiumwhitlockite and Hydroxylapatite Plasma-Sprayed Coatings in Goats, *J. Biomed. Mater. Res., 25*, (1991) 1183-120.
14. R.G.T. Geesink, K. de Groot, and C.P.A.T. Klein, Chemical Implant Fixation Using Hydroxyl-Apatite Coatings, *Clin. Orthop., 225*, (1987) 147-170.
15. C.P.A.T. Klein, P. Patka, H.B.M. van der Lubbe, J.G.C. Wolke, and K. de Groot, Plasma-Sprayed Coatings of Tetracalciumphosphate, Hydroxylapatite and Alpha-TCP on Titanium Alloy. An Interface Study, *J. Biomed. Mater. Res., 25*, (1991) 53-65.